Analysis of Be doping influence on strained GaAsP layer grown on GaAs substrate by MBE

JIAO GANG-CHENG[a,b,c,*], SHI FENG[b,c], GUO HUI[b,c], HU CANG-LU[b,c], XU XIAO-BING[b,c], ZHANG LIAN-DONG[b,c], MIAO ZHUANG[b,c], CHENG HONG-CHANG[b,c]
[a]*School of Materials Science and Engineering, Northwestern Polytechnical University, State Key Laboratory of Solidification Processing, 710072 Xi'an, China*
[b]*Science and Technology on low-light-level night vision laboratory, 710065 Xi'an, China*
[c]*North Night Vision Technology Group Co., Ltd, 650223 Kunming, China*

$GaAs_{1-x}P_x$/GaAs compound materials are used in the Negative electron affinity (NEA) III-V semiconductor photocathode for 532 nm sensitive. The author studies 880 ^oC, 900 ^oC and 920 ^oC Be cell temperature for material performance influence by HR XRD, AFM, ECV and Hall system. Below the 900 ^oC of the Be cell, the material performance were improved, which resulted in smaller surface roughness and lower threading dislocation density. Since Be doping is essential for GaAsP photocathode of GENIII imaging intensifier, these results are useful for improving the GaAsP photocathode material properties and performance of device.

(Received December 9, 2013; accepted November 13, 2014)

Keywords: GaAsP, Be doping, Molecular beam epitaxy, Crystalline quality

1. Introduction

The most sensitive photocathode available today is the Negative electron affinity (NEA) III-V semiconductor photocathode, which consists of a P-type semiconductor activated with a work function lowering Cs-O layer. The P-doping level is typical in the high 1E18 or low 1E19 cm^{-3} range so as to result in band bending. As a result, electrons generated by an incident photon exciting an electron form the valence band to the conduction band have a good probability of being emitted if they are generated within a minority carrier diffusion length of the emission surface [1-2]. It is well known that GaAsP material is also this kind of the material and can be made to NEA photocathode. It is reported that GaAsP photocathode quantum efficiency as high as 60% has been obtained. The larger band gap of GaAsP results in greater NEA and then a higher electron escaping probability [3].

The growth of $GaAs_{1-x}P_x$/GaAs compound materials is investigated widely. Unfortunately, many challenges to high-quality epitaxial growth of the $GaAs_{1-x}P_x$ materials on GaAs substrate are still existed. The most significant ones of these challenges are the process of the epitaxy growth and especially heavily P-type doping to the strained $GaAs_{1-x}P_x$ on GaAs substrate [4-10].

In order to achieve good crystalline quality and heavy P-type dopant of strained $GaAs_{1-x}P_x$ on GaAs substrate, we must well know the Be doping characteristic in strained $GaAs_{1-x}P_x$ layer and find out the optimum direction to improve the crystalline quality of the $GaAs_{1-x}P_x$/GaAs photocathode material and device performance. In the process of our research, three series of samples with various Be doping concentration of $GaAs_{0.9}P_{0.1}$ (a=5.6305Å) were fabricated on GaAs (a=5.6419Å) substrate, which was lattice mismatch of 0.2% [2]. High resolution X-ray diffractmeter, atomic force microscope, electrochemical capacitance-voltage profiler and Hall system were used to characterize the samples. The rule of the doping characteristic will be of benefit to optimum of the growth condition and helpful for obtaining the excellent crystalline quality of $GaAs_{1-x}P_x$ grown on GaAs substrate.

2. Experimental procedure

Three series of the samples were grown on epiready semi-insulation GaAs (100) substrate by using an all solid source Riber C21T system equipped with a valved arsenic and phosphorus cracker cell. The structure of the GaAsP/GaAs sample is shown in Fig. 1. Before the growth of $GaAs_{0.9}P_{0.1}$, 100 nm GaAs buffer layer was grown on the substrate, above the GaAs buffer layer, 1200 nm $GaAs_{0.9}P_{0.1}$ top layer was grown at 480°C. The concentration of three series of the $GaAs_{0.9}P_{0.1}$ layers were adjusted by Be cell temperature. The Be cell temperature for different samples were shown in Table 1. The other growth conditions of V/III ratios (10~100) and growth rate (1000 nm/h) for different samples were kept at constant. All the samples were cooled down quickly after stopping growth.

The double crystal X-ray rock curve was carried out by using Phillips MRD high resolution X-ray diffractormeter (HR XRD). HR XRD scans at (004) were made. A Ge (220) channel cut analyzer crystal was inserted before the detector in this measurement. The surface roughness of the samples was measured by the BRUKER EDGE atom force microscopy (AFM). The doping characteristic of the sample were checked by the Dage CVP 21 electrochemical capacitance-voltage (ECV) profiler. The doping concentration and mobility (300 K) of the samples were made by Hall test system.

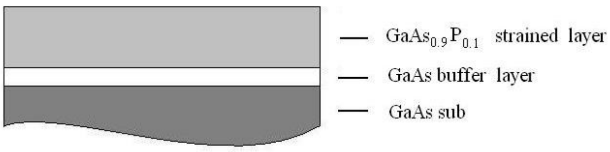

Fig. 1. Schematic diagram of $GaAs_{0.9}P_{0.1}$/GaAs sample.

Table 1. Be cell temperature for growth of various $GaAs_{0.9}P_{0.1}$/GaAs samples.

Sample number	Be cell temperature / ^{o}C
Sample A	880
Sample B	900
Sample C	920

3. Results and discussion

Fig. 2 shows a double crystal X-ray diffraction (004) rocking curves for various $GaAs_{1-x}P_x$/GaAs samples. According to Fig. 2, the peaks are corresponding to sample A, sample B, and sample C from left to right. Those sample compositions are x=0.105, 0.10, 0.116 for sample A, sample B, and sample C respectively. The full width at half maximum (FWHM) of various samples are about 647 second, 679 second, 1826 second. We can see that the crystalline quality of the samples becomes much worse with the rising of the Be cell temperature. It is said that the Be doping concentration just influences the crystalline quality, excessive Be doping can deteriorate the $GaAs_{1-x}P_x$/GaAs material performance.

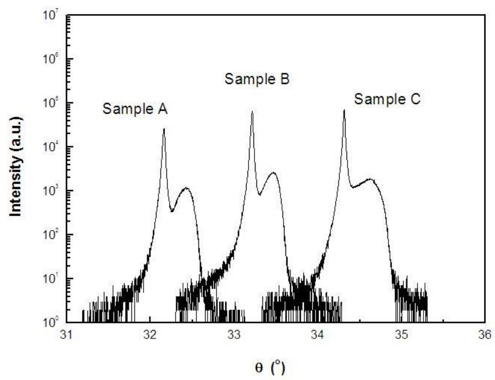

Fig. 2. HR XRD (004) rocking curves for various $GaAs_{0.9}P_{0.1}$/GaAs samples.

An atomic force microscope was used to capture the surface images of various $GaAs_{0.9}P_{0.1}$/GaAs samples. In Fig. 3, Fig. 3(a) is the sample A with Be cell temperature at 880 ^{o}C and RSM=1.69 nm, Fig. 3(b) is the sample B with Be cell temperature at 900 ^{o}C and RSM=1.98 nm, and Fig. 3(c) is the sample C with Be cell temperature at 920 ^{o}C and RSM=2.25nm. We can see the RSM of the various samples become lager with the rising of Be cell temperature. It is said that the surface quality of the $GaAs_{0.9}P_{0.1}$/GaAs samples gets worse with the increasing of Be concentration. If we want to get the P-type doping as heavy as we wish, we must optimize the growth conditions. Otherwise, the surface and crystalline quality will decrease to the bad level which can not allow to be used as photocathode emission material. This trend in the roughness of the samples is in accord with the XRD results.

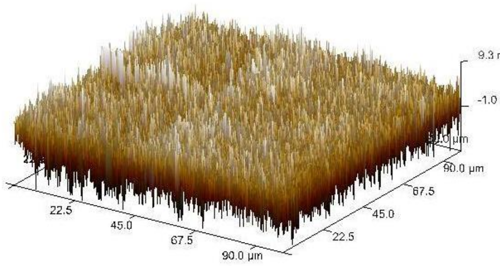

(a) Sample A with Be cell temperature 880 ^{o}C and RSM=1.69 nm

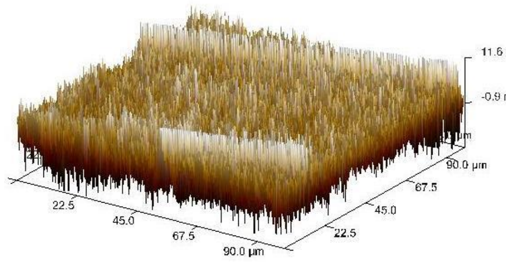

(b) Sample B with Be cell temperature 900 ^{o}C and RSM=1.98 nm

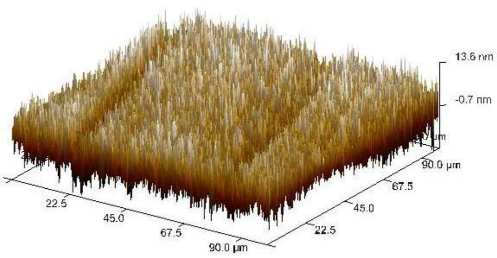

(c) Sample C with Be cell temperature 920 ^{o}C and RSM=2.25 nm

Fig. 3. AFM images of various $GaAs_{0.9}P_{0.1}$/GaAs sample surfaces.

The doping concentration of the sample was carried out by ECV profiler as shown in Fig. 4. According to the curves got by ECV profiler, the maximum concentration of sample A reached 2.69E19, sample B 5.07E19 and sample C 8.82E19 respectively. The depth of the $GaAs_{0.9}P_{0.1}$ layer for sample A and B is far more than 1.2 μm which is same as initial design. It is because of the excessive Be doping diffusing to GaAs buffer or much higher grow temperature. Thus, we should try our best to decrease the Be concentration or cool down the growth temperature in the future research.

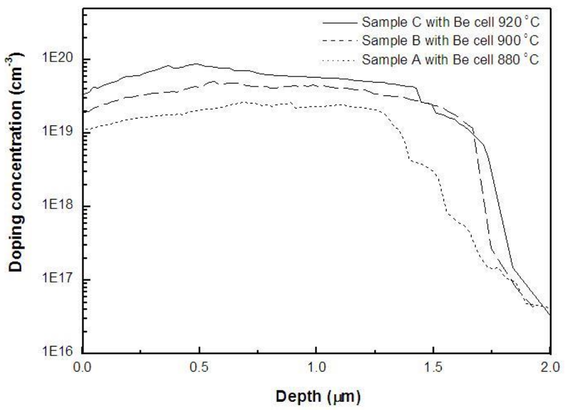

Fig. 4. ECV curves of various $GaAs_{0.9}P_{0.1}$/GaAs samples.

In order to analyze the influence of Be doping on electrical performance of the samples, Hall system is used. The test results are shown in Fig. 5. The mobility of the sample decreases with the temperature rising of Be cell. The higher doping concentration deteriorates the crystalline quality. When Be cell temperature is greater than or equal to 900 °C, the mobility of the samples decrease slowly. Thus, we must lower down the doping concentration to $GaAs_{0.9}P_{0.1}$ layer to got optimum doping concentration and improve the crystalline quality. According to the picture, we can get the concentration of sample A, sample B and sample C, whose concentration are 1.52E19, 3.32E19, 5.38E19 respectively, which is in concordance with the concentration of the samples surface.

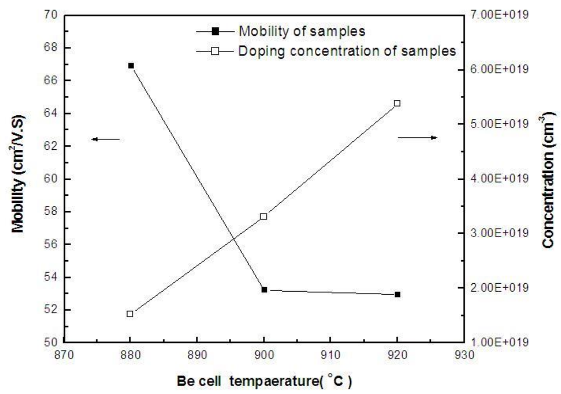

Fig. 5. Mobility and doping concentration of $GaAs_{0.9}P_{0.1}$/GaAs samples as function of Be cell temperature.

4. Conclusions

In summary, we have studied the influence of Be doping on strained $GaAs_{0.9}P_{0.1}$ layer on GaAs substrate by MBE. $GaAs_{0.9}P_{0.1}$ layer with Be doping is sensitive to the Be cell temperature. As the Be of cell temperature is at 920 °C and growth rate is 1000nm/h, the concentration reaches up to 8.82E19, as greater than or equal to 900 °C, the crystalline quality, surface quality, and mobility of the samples become worse, and phenomenon of heavy doping diffusion to substrate occurs. When Be cell temperature is 880 °C, the material properties is much better, which will result in smaller surface roughness, lower threading dislocation density and get proper doping concentration. Thus, our next step of the experiment is to decrease the Be doping concentration and optimize the doping procedure. Since Be doping is essential for GaAsP photocathode of GENIII imaging intensifier, these results are useful for improving the material properties and performance of GaAsP photocathode.

References

[1] S. M. Xiang, G. Q. Ni, National Defense Industry Publication Press, Beijing, 1999.
[2] E. K. Liu, B. S. Zhu, J. S. Luo. Semiconductor Physics, Electronic Industry Publication Press, Beijing, 2003.
[3] J. P. Edgecumbe, V. W. Aebi, G. A. Davis, Proceeding of SPIE **1655,** 204 (1992).
[4] T. H. Gfroerer, D. G. Hampton, P. R. Simov, M. W. Wanlass, J. Apl. Phy. **107**, 12379 (2010).
[5] T. J. Grassman, M. R. Brenner, M. Gonzalez, A. M. Carlin, Transactions on Electron Devices **57**, 3361 (2010).
[6] K. Hayashi, T. Soga, H. Nishikawa, T. Jimbo, M. Umeno, in Proc. 1st World Conf. Photovoltaic Energy Convers. (1994).
[7] S. S. Cetin, B. Kinaci, T. Asar, I. Kars, M. K. Ozturk, Surface and Interface Analysis, **42**, 1252 (2010).
[8] B. W. Liang, C. W. Tu, J. App. Phys. **74**, 255 (1993).
[9] S. D. Wu, L. W. Guo, W. X. Wang, Z. H. Li, Chin. Phys. Lett. **22**, 960 (2005).
[10] J. Simon, S. Tomasulo, P. J. Simmonds, M. Romero, M. L. Lee, J. Appl. Phys. **109**, 013708 (2011).
[11] R. Mosca, P. Bussei, S. Frachi, P. Frigeri, E. Gombia, J. App. Phys. **93**, 9709 (2003).

*Corresponding author: jiaogc613@163.com